



## Identification of a slight vortex induced vibration episode at the Grande Ravine Viaduct

Fernando Bastos, Elsa Caetano, Alvaro Cunha, Xavier Cespedes, Olivier Flamand

### ► To cite this version:

Fernando Bastos, Elsa Caetano, Alvaro Cunha, Xavier Cespedes, Olivier Flamand. Identification of a slight vortex induced vibration episode at the Grande Ravine Viaduct. 7th European-African Conference on Wind Engineering (EACWE 2017), Jul 2017, Liège, Belgium. hal-02309677

**HAL Id: hal-02309677**

**<https://cstb.hal.science/hal-02309677>**

Submitted on 9 Oct 2019

**HAL** is a multi-disciplinary open access archive for the deposit and dissemination of scientific research documents, whether they are published or not. The documents may come from teaching and research institutions in France or abroad, or from public or private research centers.

L'archive ouverte pluridisciplinaire **HAL**, est destinée au dépôt et à la diffusion de documents scientifiques de niveau recherche, publiés ou non, émanant des établissements d'enseignement et de recherche français ou étrangers, des laboratoires publics ou privés.

## IDENTIFICATION OF A SLIGHT VORTEX INDUCED VIBRATION EPISODE AT THE GRANDE RAVINE VIADUCT

Fernando BASTOS<sup>1</sup>, Elsa CAETANO<sup>1</sup>, Álvaro CUNHA<sup>1</sup>, Xavier CESPEDDES<sup>2</sup>, Olivier FLAMAND<sup>3</sup>

<sup>1</sup>VIBEST/CONSTRUCT - University of Porto, Faculty of Engineering – Portugal

<sup>2</sup>SETEC.tpi – France

<sup>3</sup>CSTB – France

[fjbastos@fe.up.pt](mailto:fjbastos@fe.up.pt), [ecaetano@fe.up.pt](mailto:ecaetano@fe.up.pt), [acunha@fe.up.pt](mailto:acunha@fe.up.pt), [olivier.flamand@cstb.fr](mailto:olivier.flamand@cstb.fr)

*The work here presented results from the study of the monitored data collected during a 2-year period at the viaduct of Grande Ravine at the Reunion Island. Based on the records collected by a set of anemometers, pressure sensors and accelerometers, it was possible to establish a wind model for the Grande Ravine implantation site, to estimate force coefficients for the deck, and to identify modal properties (vibration frequencies, damping and modal configurations). From the analysis of the structural response, it was possible specifically to identify a case of very slight vortex induced vibration, which is described in detail in this paper.*

Keywords: Full-scale monitoring, bridge aerodynamics, vortex-induced vibration

### THE GRANDE RAVINE VIADUCT: STRUCTURE AND MONITORING SYSTEM

The permanent concerns of the scientific and engineering community with the structural health and safety of bridges, due to the increase of audacious design solutions involving longer and longer spans and very slender structural systems, have led to the instrumentation of a significant number of bridges with continuous monitoring systems. Many of these structures are located in zones with high susceptibility to the occurrence of extreme events, such as cyclones, demanding an adequate characterisation of loads and an accurate assessment of the corresponding response. The Grande Ravine viaduct is a slender girder bridge crossing a volcanic breach of 320m width and 170m depth, at the Reunion Island. The steel orthotropic deck is 288m long and 22.7m width and is supported by two concrete struts, inclined at 20° with horizontal, fixed in a concrete abutment founded in solid rock (Fig. 1).

The viaduct is located in an area frequently affected by tropical cyclones and, due to a particular concern regarding the understanding of the corresponding wind response, the Designer SETEC tpi decided to install a continuous monitoring system. This system includes 5 anemometers (Fig 1b), 14 pressure sensors distributed along the contour of two cross sections (Fig. 1c and 1d), 6 temperature sensors, and 6 accelerometers, arranged in 3 pairs in transversal and vertical direction of 3 cross sections (Fig. 1b). Collaboration between the Designer, ViBest/FEUP and CSTB was established in order to process and analyse the recorded data, aiming at validating the wind studies carried out during the design stage.

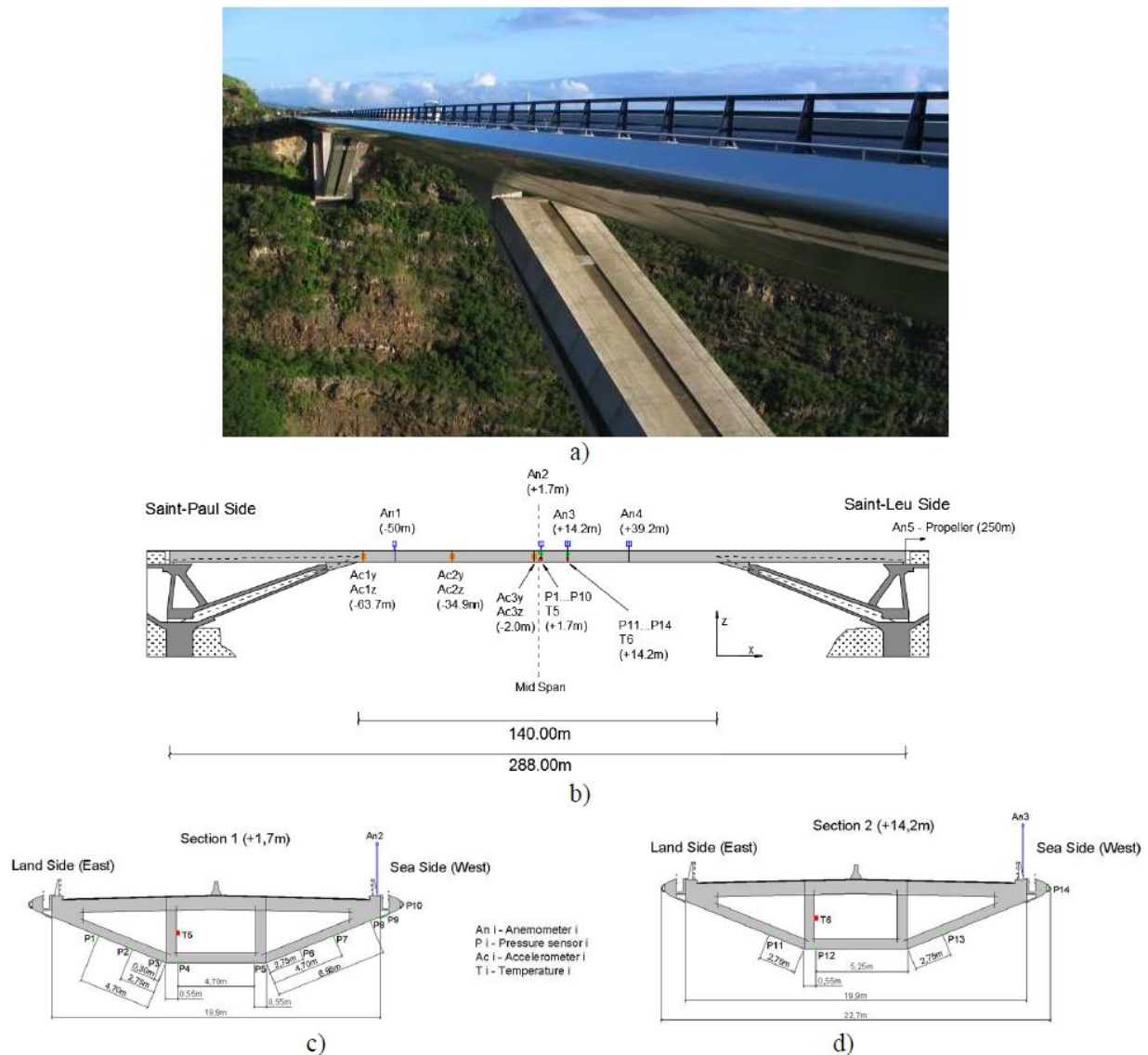


Fig. 1– Scheme of instrumentation: (a) distribution of sensors along the viaduct profile; (b) pressure sensors in section 1, +1,7m from mid-span; (c) pressure sensors in section 2, +14,2m from mid-span.

### Structural Response: Identification of modal parameters based on full-scale measurements

The signals synchronously measured by the different sensors were sampled at 40Hz and stored in a computer located at the bridge site. The raw data files were then downloaded via FTP and stored in a computer at FEUP (Porto). Subsequently, these files were subjected to a pre-processing treatment including the removal of spikes and possible offsets introduced by power supply or the measurement chain, and a decimation to 20Hz, followed by a packaging into 1-hour data files for further processing. The application of an automated version of p-LSCF identification algorithm [1] to the acceleration data collected at the Grande Ravine viaduct during a 2-year period allowed to obtain a very reliable characterisation of the time evolution of the structure modal parameters. Fig. 2 shows the evolution of the bridge first 11 natural frequencies during the period under analysis. Table 1 presents the mean, minimum and maximum values of the first 11 frequencies and corresponding identified damping ratios. The modal configurations of the first two vibration modes are presented in Fig. 3. A more detailed study of the time variation of modal properties can be found in [2].

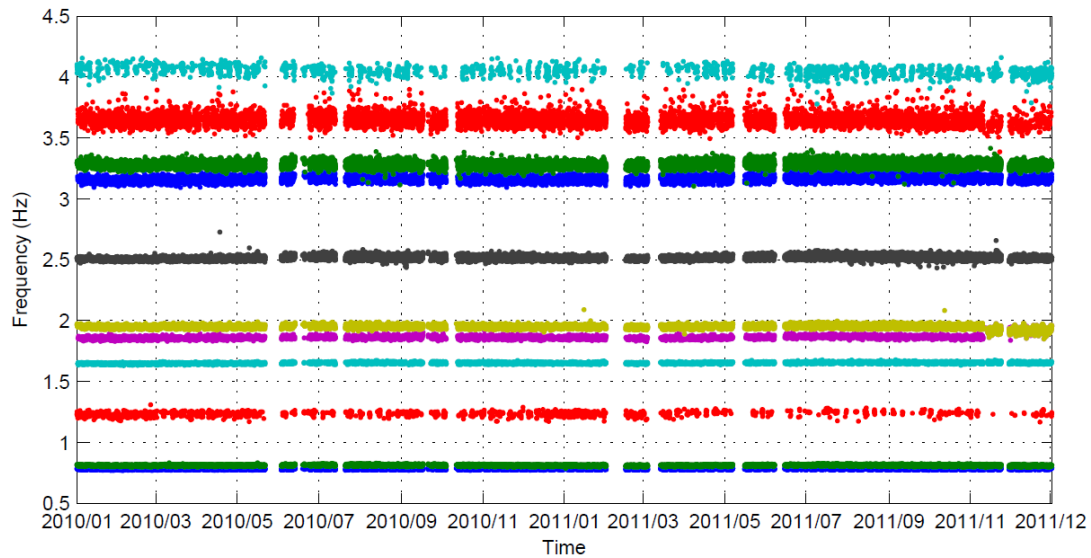
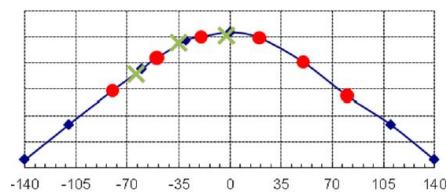


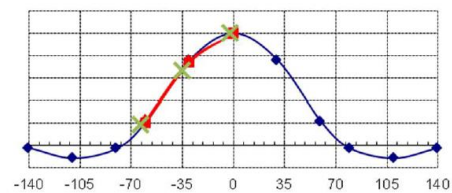
Figure 2 – Variation of the viaduct first 11 natural frequencies identified with the *p*-LSCF method in the 2-years monitoring period after grouping of modes.

Table 1 – Results of the *p*-LSCD method for the monitoring period under analysis

Mode	$f_{\text{mean}}$ (Hz)	$f_{\text{min}}$ (Hz)	$f_{\text{max}}$ (Hz)	$\xi_{\text{mean}}$ (%)	$\xi_{\text{min}}$ (%)	$\xi_{\text{max}}$ (%)	Modal configuration
1	0.7818	0.7681	0.7969	0.98	0.04	2.11	transversal
2	0.8114	0.7859	0.8325	1.11	0.10	2.73	vertical
3	1.2348	1.1673	1.3089	1.93	0.05	5.70	vertical
4	1.6507	1.6310	1.6773	0.51	0.02	1.24	transversal
5	1.8693	1.8256	1.9891	0.73	0.01	2.92	vertical
6	1.9506	1.8506	2.0902	1.31	0.08	2.92	vertical
7	2.5175	2.4338	2.7277	1.17	0.10	4.32	torsion
8	3.1649	3.0933	3.3280	0.74	0.02	2.47	transversal
9	3.2848	3.1044	3.4159	1.47	0.07	3.98	vertical
10	3.6450	3.3872	3.9012	1.56	0.10	5.07	vertical
11	4.0497	3.7784	4.1607	1.02	0.01	4.96	torsion



a) 1<sup>st</sup> transversal  
( $f_{\text{req}}=0.782\text{Hz}$ )



b) 1<sup>st</sup> vertical  
( $f_{\text{req}}=0.811\text{Hz}$ )

Figure 3 – Modal configurations of the first two vibration modes: a) 1<sup>st</sup> transversal and b) 1<sup>st</sup> vertical (in blue numerical, red ambient vibration test and green continuous monitoring).

## IDENTIFICATION OF ONE EPISODE OF VORTEX INDUCED VIBRATION

This section focuses on the study of vortex-induced vibrations (VIV) with emphasis to phenomena of this nature captured during the continuous monitoring period of the viaduct of Grande Ravine. This type of phenomena occurs as consequence of harmonic excitation of the first vertical (or torsional) vibration mode of the deck due to the release of vortices in the wake of the section at a frequency

close to a fundamental frequency of the structure. Given the geometry of the section of the deck, and due to the inclined walls and to the proximity of frequencies of the first horizontal and vertical modes, vortex induced vibrations can also be observed associated with the horizontal mode, although with a much more discrete response.

Generally, VIV episodes are of very short duration, stemming from the combination of a number of factors, which do not easily coexist. Apart from this fact, the observation of VIV is rare, since structures are studied in order to ensure the smallest possible impact on their users daily life, ie, to prevent the manifestation of such events with amplitudes perceptible to the users or that incur into structural fatigue. The most important factors for the occurrence of VIV phenomena are the range of potentially excitable wind speeds (directly proportional to the shedding frequency) and the ideal conditions of atmospheric turbulence in order to maintain the eddy flow structures.

VIV episodes are governed by the frequencies with which the vortices are released in the wake of the flow [3]. These frequencies are related with the Strouhal number, a dimensionless quantity which varies from body to body depending on the velocity and on the geometry of the body immersed in the flow [3, 4].

The occurrence of VIV is widely described in the literature [3, 4, 5], standing out some famous cases of bridges, namely the Great Belt Bridge or even the well-known case of Tacoma Bridge where vibrations were initiated by of vortex shedding at low wind speed and rapidly converged to a flutter phenomenon. In this context, the investigation of such phenomena requires the definition of a set of strategies that lead to the detection of events with characteristics compatible with those required for the occurrence of vortex-induced vibrations. In order to identify these phenomena, a first criterion has been established based on the observation of the correlation between the recorded acceleration amplitudes (through the rms value) and the mean wind velocity. Accordingly, the definition of the data sampling period for which the statistical properties are calculated is of extreme importance: it should not be set too short, so as not to suffer the effects of traffic influence on the viaduct and, at the same time, it should not be too long to be influenced by the turbulence of the global flow. Thereby the interval of 30 seconds was defined as the experimental sampling period to observe this phenomenon. On the other hand, based on the wind tunnel estimates obtained for the Strouhal number [2], knowing the range of possible velocities for the occurrence of this phenomenon, the events contained in the range of speed conducting to higher probability of occurrence of VIV phenomena were selected. Fig. 4 shows the variation of horizontal and vertical vibration amplitude (rms values) recorded by the accelerometers with the mean wind velocity based on averaging intervals of 30s.

The observation of this figure shows a cloud greatly influenced by traffic on the bridge. However, a set of points stand out from the overall, especially in the range of the highest mean wind velocity and with the same order of magnitude expected for the occurrence of such events.

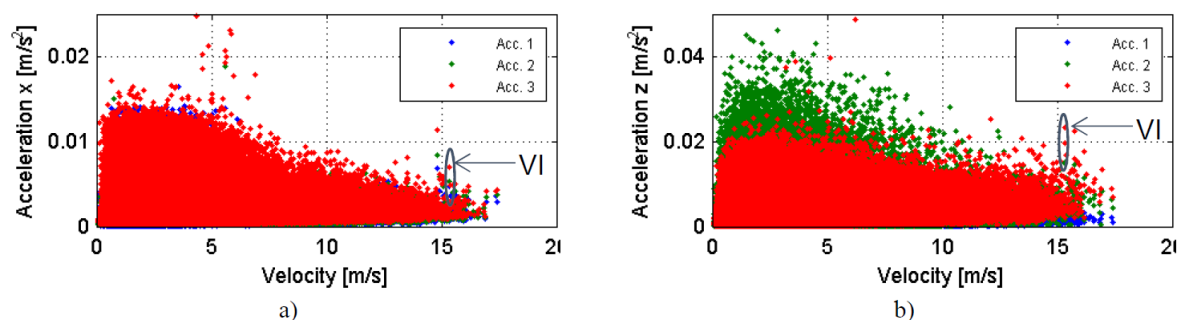


Figure 4 – Variation of rms values of (a) horizontal and (b) vertical acceleration with mean wind velocity for averaging intervals of 30 seconds.

## Characterisation of VIV phenomena

The analysis of time series corresponding to the points marked in Fig. 4 allows to observe the building of a low amplitude harmonic vibration. This is evident from the observation of Fig. 5 displaying the horizontal and vertical acceleration time series at the viaduct mid-span.

The time interval analysed corresponds to a Sunday between 17:34:27 and 17:37:02, coinciding with a period of low traffic occurrence.

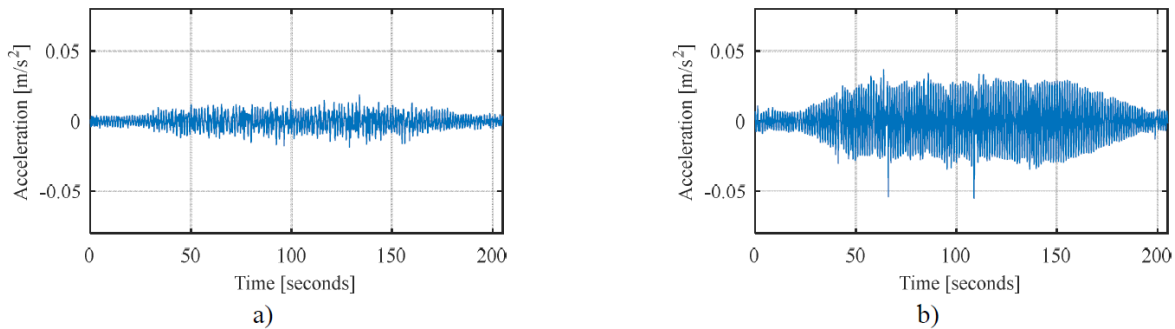


Figure 5 – Time-histories of (a) horizontal and (b) vertical acceleration during the period under analysis.

Fig. 6 shows a zoom of the signals presented in previous Fig. 5. This graph denotes a pattern of response purely dominated by a singular frequency, which is confirmed by observation of the spectral estimates of the acceleration signals shown in Fig. 7.

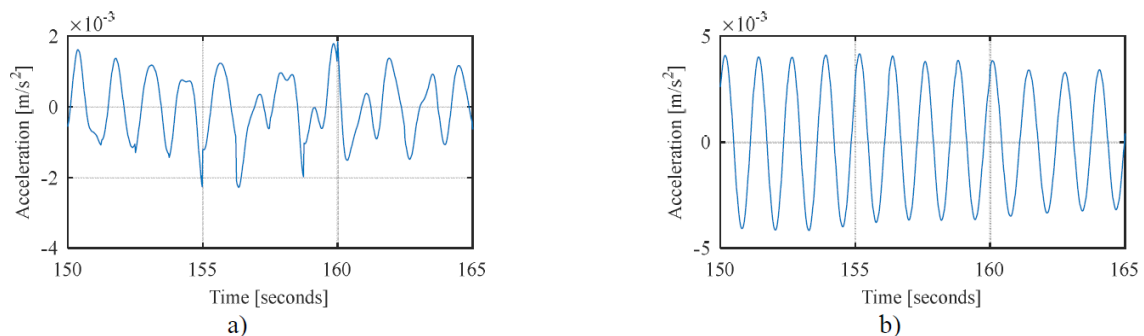


Figure 6 – Zoom of time-history signals of (a) horizontal and (b) vertical acceleration of figure 7.57.

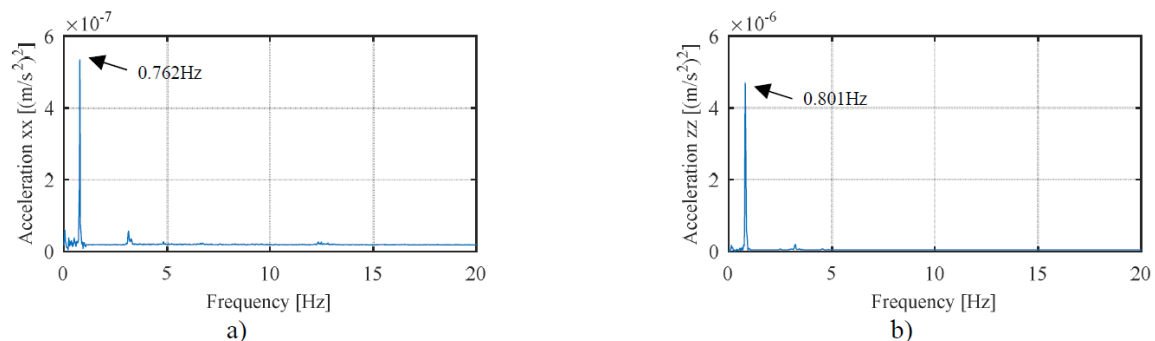


Figure 7 – Spectral estimates of time-histories of (a) horizontal and (b) vertical acceleration.

The peaks observed in the spectral estimates of the horizontal and vertical acceleration signals correspond to the excitation of the 1st vertical vibration mode of the deck. Response in the 1st horizontal mode can also be observed in Fig. 7a), although with a slightly smaller amplitude than that associated with the 1st vertical vibration mode. The remaining vibration modes have a negligible contribution to the structural response.



It is also observed that during the period of analysis no traffic existed on the viaduct, and thereby the records of the acceleration have no response due to the vehicle passage and particularly the impulse due to the entrance of vehicles on the viaduct.

These facts evidence the importance of characterising the wind synchronously with the presented events. Fig. 8 shows the time series of the wind direction, and the horizontal and vertical velocity components for the analysed time interval.

The data shown in Fig. 8 evidence a very stable pattern, ie, quasi-constant horizontal velocity and direction. Table 2 summarises the statistical properties of the signals illustrated in Fig. 8.

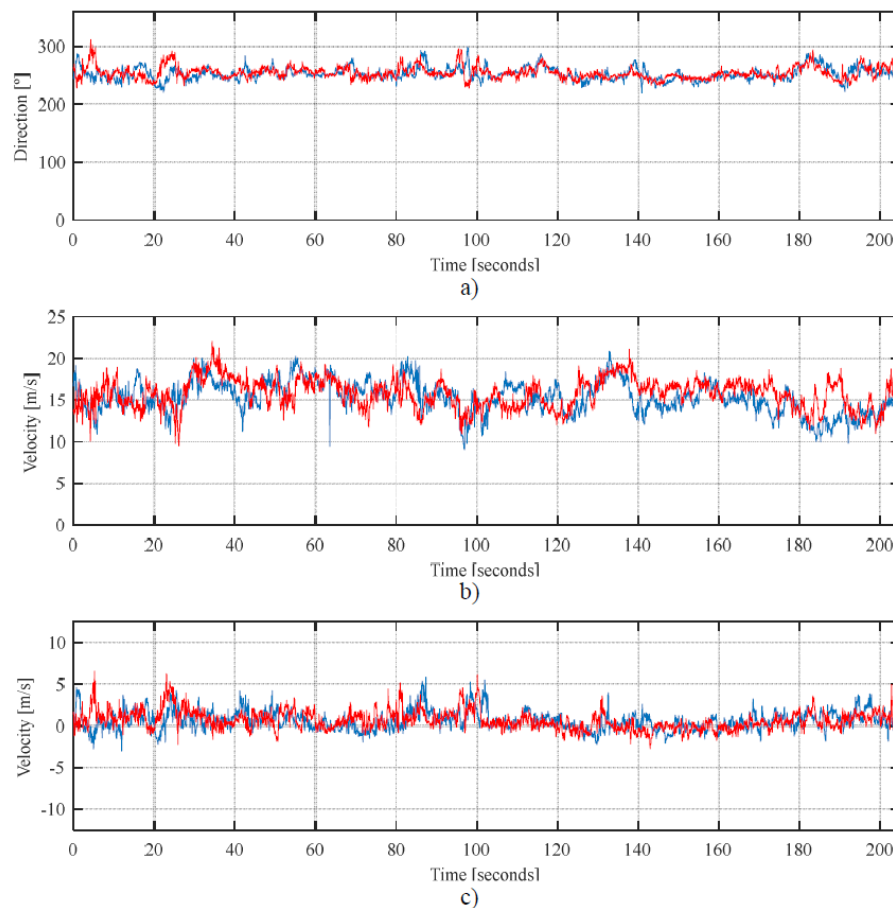


Figure 8 – Time-histories of wind (a) direction and velocity in (b) horizontal and (c) vertical directions during the period of 235 seconds.

Table 2 – Statistical parameters from wind time histories presented in Figure 8, corresponding to a time interval of 215seconds.

	Anemometer 2	Anemometer 3
Mean velocity U [m/s]	15.36	15.58
Direction d [°]	254.33	256.62
Incidence i [°]	0.93	0.87
Iu	0.116	0.118
Iw	0.068	0.067

The velocity values shown in this Table are in the potentially excitable range of 15m/s to 19 m/s identified from wind tunnel tests in the context of the estimation of the Strouhal number [2]. The analysed time histories present lower turbulence intensity than that estimated in the context of characterisation of the atmospheric and aerodynamic properties of Grande Ravine viaduct site [2]. For

very high wind conditions in which the pattern of atmospheric behaviour tends to homogeneity, turbulence intensity values may be very similar to the values observed for these time series.

It is also noted that during the observed period wind has ascending incidence and direction from the sea, almost normal to the viaduct. These characteristics are similar to those observed for the occurrence of higher intensity wind in the characterisation of local wind properties.

Fig. 9 presents the spectral estimates of the velocity time series shown in Fig. 8. These estimates have a similar configuration to those obtained in the detailed study of wind properties characterisation [2]. However, slightly higher values of turbulence scales are observed in the present records.

Aiming at characterising a possible vibration episode induced by vortex shedding, the pressure signals recorded at the contour of the deck section during the observation period were analysed. Fig. 10 shows the temporal signals at the sensors P10 and P3, positioned under direct incident wind and in the wake of the cross section, respectively (see Fig. 1 c d)). A zoom of such records in a narrow time interval is shown in Fig. 11. Spectral estimates of these records are presented in Fig. 12.

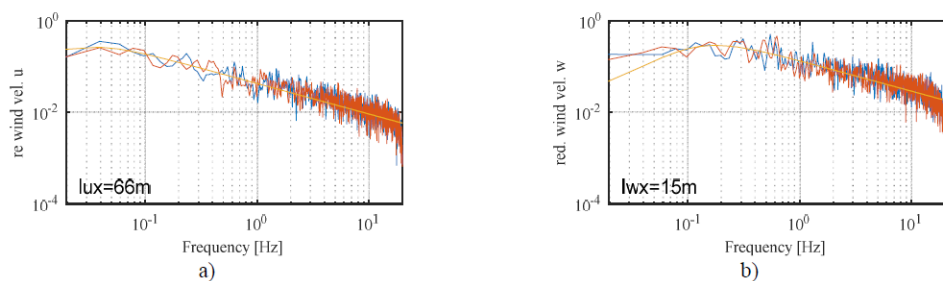


Figure 9 – Spectral estimates of (a) longitudinal and (b) vertical components of wind velocity during the period under analysis. In blue the von Karman theoretical spectral function.

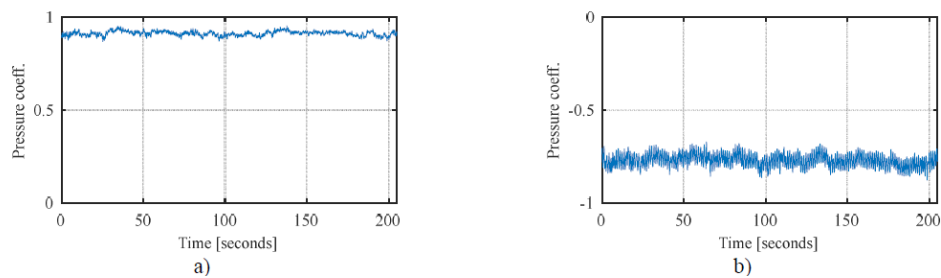


Figure 10 – Time-histories of pressure measured at sensors (a) P10 and (b) P3 during the time interval under analysis.

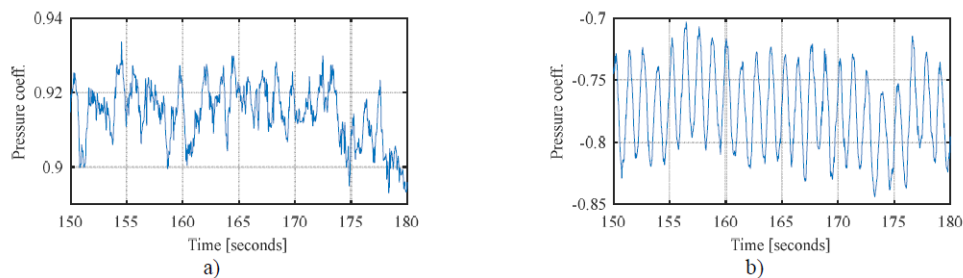


Figure 11 – Time-histories of pressure measured at sensors (a) P10 and (b) P3 during the time interval under analysis



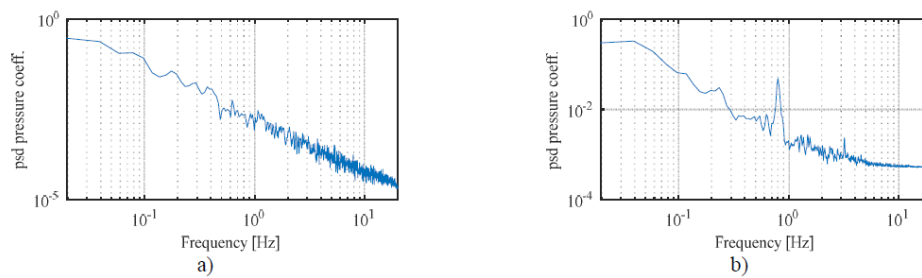


Figure 12 – Spectral estimates of pressure records at sensors (a) P10 and (b) P3.

The observation of Figs. 11 and 12 shows that the signal recorded by the pressure sensor P3, positioned in the wake of the cross section, presents a strong harmonic component characterised by a frequency associated to the release of vortices in the wake of the section. The rate of vortex release is close to the frequency of the first vertical mode of the deck. In the case of the signal measured at the pressure sensor P10, positioned under incident wind, the reported harmonic component is almost imperceptible.

Still in the context of the analysis of the aerodynamic forces generated in the section contour, Fig. 13 shows the spectral estimates of the aerodynamic forces  $F_x$  and  $F_z$  derived from the integration of the pressures along the contour of the viaduct cross section [2].

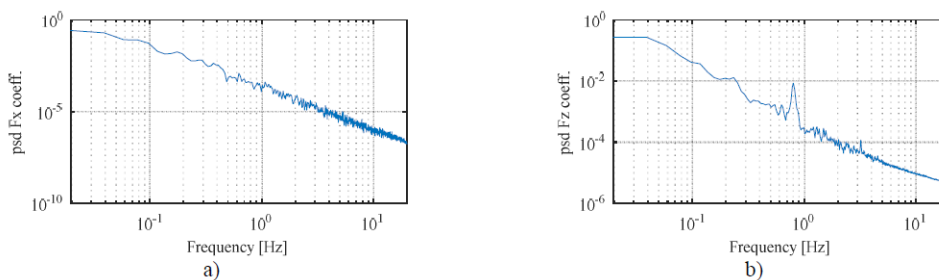


Figure 13 – Spectral estimates of the estimated (a) drag and (b) lift forces during the period under analysis.

The graph representing the spectral estimate of the lift force clearly shows a peak associated to vortex shedding. With respect to the spectral estimate of the drag force, a very tenuous peak can be observed, being this component of aerodynamic force essentially dominated by incident turbulence. This peak results from the pressure integration along the inclined walls of the cross section.

### Estimation of the Strouhal number from full-scale measurements

At this moment, it becomes pertinent to estimate the Strouhal number ( $St$ ) based on the frequency ( $n$ ) estimated from the peak found in Fig. 13, the mean wind velocity ( $U$ ) and the reference dimension  $B$  (width) of the deck, according to the equation ( $St = n.B/U$ ). Considering the values presented in Table 2, estimates of  $St$  range from 0.206 to 0.213. These estimates, summarised in Table 3, are very similar to those based on wind tunnel tests. Although extremely close, the differences can be justified by the different turbulence conditions between the prototype and the model.

Table 3 – Strouhal number: estimates based on wind tunnel and full-scale measurements.

Experimental Uniform(CSTB [6], Bastos [2])	0.210
Experimental Turbulent(CSTB[6], Bastos [2])	0.186
Full-scale measurements	0.206-0.213

During the occurrence of VIV events, the increase of coherence between time series of pressure measured in contiguous points is expected. This occurs due to the synchronization of vortices released from the surface of the cross sections and structural natural frequency. This type of occurrence was described by several authors from tests conducted in wind tunnel [4,7] and also reported in the context of the analysis of the wind tunnel test results [2]. In order to test this hypothesis for the full-scale approach, Fig. 14 shows the estimates of coherence functions between pressures measured in contiguous sensors P10-P14 (incident wind) and P3-P11 (wake flow) (see location in Fig. 1c and 1d).

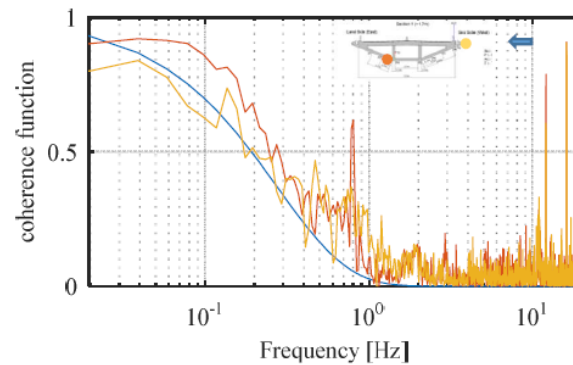


Figure 14 – Coherence estimates between pressure sensor signals (a) P10-P14 (in yellow) and P3-P11 (in orange) recorded during the period under analysis. Theoretical decay exponential coherence function (in blue) of longitudinal wind component based on the parameters of Table 1.

The observation of this figure evidences a very tenuous increase of coherence in the case of the sensors positioned under direct influence of the wind (P10 and P14). In the case of sensors placed on the wake of flow (P3 and P11) notorious increase is observed.

## FINAL REMARKS

Considering the results above presented for the overall pattern described in literature, it can be concluded that a vortex induced vibration event has occurred.

It is noted that, during the conception studies, it was observed that the Grande Ravine cross section, was susceptible to developing vortex shedding. This observation was first evidenced from the shape of the lift coefficient graph, presenting a negative slope, and subsequently confirmed by the configuration of the H1 aerodynamic derivative associated to the vertical damping component developed as consequence of aerodynamic forces on the deck, which presents a positive portion [2]. This observation was registered for low reduced velocities, with an intensity of velocities of the same order of those in which the vortex induced vibration was observed for the prototype.

The occurrence of vortex induced vibration requires the simultaneous presence of a number of factors, which probability of occurrence by themselves is very low. For this reason, the difficulty in finding the phenomena observed in this case study is a result of the decisions regarding the deck geometry taken during the design stage, in order to avoid the occurrence of vibratory phenomena with aerodynamic character. It should be noted that the constant high intensity traffic observed and the topographic condition are factors that can destabilise the possible mechanism of formation of these vortices, by increasing the turbulence near the walls of the viaduct cross section. In fact, it is very difficult to find the simultaneous condition of low turbulence intensity, low traffic on the viaduct, constant incidence and direction and, most important, wind intensity in the favourable range, in accordance with the Strouhal number, for the occurrence of harmonic vibrations due to vortex shedding synchronised with the natural frequencies of the structure.

## Acknowledgements

The present work has been developed in the context of a collaboration established between the University of Porto and the office SETEC.tpi, responsible for the design and installation of the monitoring system at the viaduct site. Additional cooperation has been established with CSTB. This work was financially supported by: Projects POCI-01-0145-FEDER-007457 - CONSTRUCT - Institute of R&D In Structures and Construction and PTDC/ECM-EST/2110/2014 - Dyncatline , funded by FEDER funds through COMPETE2020 - Programa Operacional Competitividade e Internacionalização (POCI) – and by national funds through FCT - Fundação para a Ciência e a Tecnologia; The first author acknowledges the PhD scholarship (SFRH/BD/46126/2008).

## REFERENCES

- [1] F. Magalhães, 2010, *Operational Modal Analysis For Testing And Monitoring of Bridges And Special Structures*, FEUP, Porto, Portugal.
- [2] F. Bastos, 2015, *Aerodynamic Behaviour of Long Span Structure. Numerical Analysis and Experimental Validation Based on Full-Scale Measurements*, FEUP, Porto, Portugal.
- [3] C. Cremona, J.-C. Foucriat, 2002, *Comportement au vent des ponts.*, Presses de l'école nationale des Ponts et Chaussées, Paris, France.
- [4] E. Simiu, R.H. Scanlan, 1996, *Wind Effects on Structures: Fundamental and Applications to Design.*, John Wiley & Sons, Third Edition ed, New York, US.
- [5] Y. Fujino, K. Kimura, H. Tanaka, 2012, *Wind Resistant Design of Bridge in Japan: Developements and practices*, Springer.
- [6] J. Vinet, S. Bodere, D. Voisin, G. Grillaud, 2002, *EN-CAPE 02.152 C-V0 - Etude Aérodynamique des Ouvrages D'Art de la Route des Tamarins : coefficients aérodynamiques des viaducs des Trois-Bassins, solution Paille-en-Queue, et de la Grande Ravine.*, CSTB, Nantes, France.
- [7] C. Dyrbye, S.O. Hansen, 1997, *Wind Loads on Structures*, John Wiley & Sons, New York, US.